Tanzania Journal of Science 50(2): 224-243, 2024
ISSN 0856-1761, e-ISSN 2507-7961

The Analysis of a Co-Dynamic Ebola and Malaria Transmission Model Using the Laplace Adomian Decomposition Method with Caputo Fractional-Order

Akeem Olarewaju Yunus[1, 2*] and Morufu Oyedunsi Olayiwola [1].
[1] *Department of Mathematical Sciences, Faculty of Basic and Applied Sciences, Osun State University, 210001, Osogbo, Osun State, Nigeria, Osun State.*
[2] *Department of Mathematics and Statistics, Osun State College of Technology, Esa-Oke.*
Email address: akeem.yunus@oscotechesaoke.edu.ng, olayiwola.oyedunsi@uniosun.edu.ng.
*Corresponding Author: akeem.yunus@oscotechesaoke.edu.ng
Received 17 Aug 2023, Revised 16 Apr 2024, Accepted 25 Jun 2024, Published 30 Jun 2024
https://dx.doi.org/10.4314/tjs.v50i2.5

Abstract

The study presents a novel mathematical framework for addressing Ebola and malaria concerns in Sub-Saharan Africa that combines Laplace transformation with Caputo fractional order derivative. It takes into account socioeconomic aspects that influence disease dynamics and uses the basic reproduction number to quantify transmission dynamics. Extensive numerical simulations using Maple 18 software are used to investigate the effect of fractional order derivatives on disease dynamics. It shows how the Laplace-Adomian decomposition approach simplifies nonlinear equations and generates control solutions. It emphasizes the necessity of turning discoveries into concrete plans and encourages stakeholders to be proactive in implementing them. Overall, the study emphasizes the importance of proactive disease management measures and the promise of novel approaches to treating infectious diseases. Stakeholders may create a more resilient response to these health emergencies by working together to adopt these measures.

Keywords: Co infection Malaria -Ebola; Caputo's fractional derivative; Laplace-Adomian Decomposition Method

Introduction

The mathematical model utilizes symbols, equations, and notation to model real-world phenomena, aiding understanding, research, and drawing conclusions. Epidemiology employs mathematical models to study, forecast, and manage disease outbreaks, such as the malaria-Ebola coinfection. Fractional-order modeling, incorporating Caputo derivatives and Laplace transformations, is increasingly significant. The Laplace-Adomian approach, used in previous studies Ahmed et al. (2020), Bahaa (2017), Dokuyucu and Dutta (2020), Hassan et al. (2019), Haq et al. (2018), Yunus et al. (2022) provides convergent solutions. Pandemics, affecting large populations across continents, have been extensively studied Abdilraze and Pelinosky (2011), Ali et al. (2021), Ndairou et al. (2021), Amir et al. (2018), Muhammad et al. (2020), The field of modeling infectious disease in the early 1990 by Reiner Jr et al. (2013). Hassan et al. (2019) experimented with the model's findings to better understand parameter behavior. Mtisi et al. (2009) studied HIV/AIDS and malaria co-evolution with differential equations, focusing on female Anopheles mosquitoes transmitting the Plasmodium falciparum parasite.Yunus et al. (2023) simulated Lassa fever, suggesting controlling contact rates with alpha 1 as the most effective strategy, showcasing the model's reliability. Ebola modeling incorporates fractional derivatives (Caputo and Fabrizio) and perturbation methods Sinan and Khan (2020). Another study by Mahdy (2022), Mahdy et al. (2021), Amir et al. (2018), and Pinto et al. (2013) estimates a nonlinear model representing physiological responses. Chakraverty et al. (2020) categorized uncertainties into interval or fuzzy types, aiding management by researchers. Matsebula and Nyabadza (2022) explored LF and malaria burdens in Sub-Saharan Africa, using the Mittag-Leffler kernel to model their co-infection. Alaje et al. (2022), Arqub and Ajou (2013) evaluate the homotopy analysis method (HAM) for solving fractional order problems, enabling straightforward adjustment of the convergence region using an auxiliary parameter. Mukandavire, Z et al. (2009) deterministic model analyzes HIV-malaria interaction with stable equilibria and backward bifurcation. Mathematical models inform co-epidemic management Mutua et al. (2015), Oguntolu et al. (2022). Ongoing research seeks to improve interventions for Malaria and Ebola Omoloye and Adewale (2021). The coinfection model bears significant biological implications, guiding public health policies globally.

Preliminaries

We provide some fundamental definitions of characteristics used in the work in this section.

Definition 1:[Yunus et al (2023)**]** Fractional integration of order Riemann-Liouville $\alpha \geq 0$ positive real function $f(y) \in Q_{\mu}$, $\mu \geq -1$ $y > 0$ is defined as:

$$D^{\alpha} f(y) = \frac{1}{\Gamma(\alpha)} \int_0^t (y-t)^{\alpha-1} f(y) dy \text{ Such that } D^0 f(y) = f(y).$$

Definition 2: [Yunus et al (2023)] A positive real function's fractional Caputo derivative $f(x)$ given as $D^{\alpha} f(x)$ is given by

$$D^{\alpha} f(x) = \frac{1}{\Gamma(n-1)} \int_0^t (x-t)^{n-\beta-1} f^{(n)}(t) dt \text{ For}$$

$$n-1 < \alpha \leq n, \; n \in N, \; t > 0, \; \varphi \in Q_{-1}^{n}.$$

Definition 3: [Yunus et al (2023)] Laplace Transform Let $f(t)$ be a function defined for all positive real number $t \geq 0$ $F(s):$ $f(s) = \int_0^{\infty} e^{-st} f(y) dy$

$$L[f^{\alpha}(y)] = s^{\alpha} L[f(y)] - s^{\alpha-1} f(0) - s^{\alpha-2} f'(0) - s^{\alpha-3} f''(0) \cdots$$

The inverse Laplace transforms of $\frac{f(s)}{s}$ is $L^{-1} \frac{f(s)}{s} = \int_0^t f(y) dy$

Laplace transform of the fractional integral and derivatives for $\alpha > 0$ is defined as:

$$L[D_t^{\alpha} f(x)] = L\left[\frac{1}{\Gamma(n-\alpha)} \frac{d^n}{dx^n} \int (x-u)^{n-\alpha-1} f(x) dx \right]$$

Definition 4: [Yunus et al. (2023)] The Adomian polynomials writing as $A_0, A_{1,\ldots} A_n$, consists in the decomposition the unknown function $y(t)$ in a series of the form $y(t) = y_0 + y_1 + y_2 + \cdots y_n$ can be expressed as: $A_n = \frac{1}{n} \frac{d^n}{d\lambda^n} \left[G(t) \sum_{j=0}^{n} y_j \lambda^j \right]_{\lambda=0}$

Model Formulation and Analysis

The new fractional Caputo derivative model is established as follows: by formulating the system that develops fractional ordinary differential equations and replacing the traditional derivative with the Caputo derivative, as presented by Omoloye and Adewale (2021).

$$\left.\begin{aligned}
&{}^{c}D^{\psi_1}S_H = L\{\pi_H - \lambda_E S_H - \lambda_M S_H - \lambda_{EM} S_H - \mu S_H + \phi_1 R_M + \alpha\theta J\},\\
&{}^{c}D^{\psi_2}L_E = L\{\varepsilon_1\lambda_E S_H - (K_E + \sigma_1 + \mu)L_E + \phi_2 I_T + (1-\alpha)\theta J - (1-\rho)\phi_3 I_{EM}\},\\
&{}^{c}D^{\psi_3}I_U = L\{(1-\varepsilon_1)\lambda_E S_H + \omega_1 K_E L_E - (\gamma_{UE} + \mu + \delta_{UE})I_D\},\\
&{}^{c}D^{\psi_4}I_D = L\{(1-\omega_1)K_E L_E - (\tau_1 + \mu + \delta_{ED} + \sigma_2)I_D + \gamma_{UE} I_U + \tau_4 E_{EM}\},\\
&{}^{c}D^{\psi_5}I_T = L\{\tau_1 I_D - (\phi_2 + \mu)I_T\}, \quad L\{{}^{c}D^{\psi_6}J\} = L\{\sigma_1 L_E + \sigma_2 I_D - (\mu + \delta_J)J - \theta J\},\\
&{}^{c}D^{\psi_7}E_M = L\{\varepsilon_2\lambda_M S_H - (K_M + \mu)E_M - \tau_2 E_M + \rho\phi_3 I_{EM}\},\\
&{}^{c}D^{\psi_8}I_M = L\{(1-\varepsilon_2)\lambda_M S_H + K_M E_M - (\tau_3 + r + \delta_{IM} + \mu)I_{EM}\},\\
&{}^{c}D^{\psi_9}R_M = L\{\varepsilon_2 E_M - \tau_3 I_M + r I_M - (\phi_1 + \mu)R_M\},\\
&{}^{c}D^{\psi_{10}}E_{EM} = L\{\varepsilon_3\lambda_{EM} S_H + (K_{EM} + \delta_{JEM} + \mu)E_{EM} - \tau_4 E\},\\
&{}^{c}D^{\psi_{11}}I_{EM} = L\{(1-\varepsilon_3)\lambda_{EM} S_H + K_{EM} E_{EM} - (\phi_3 + \delta_{JEM} + \mu)I_{EM}\},\\
&{}^{c}D^{\psi_{12}}S_V = L\{\pi_V - \lambda_V S_H - \mu_V \delta_V\}, \quad L\{{}^{c}D^{\psi_{13}}E_V\} = L\{\lambda_V S_V - (\sigma_V + \mu_V)E_V\},\\
&{}^{c}D^{\psi_{14}}I_V = L\{\sigma_V E_V - \mu_V I_V\}.
\end{aligned}\right\} \quad (1)$$

With given initial condition $S_{H_0} = m_1, L_{E_0} = m_2, I_{U_0} = m_3, I_{D_0} = m_4, I_{T_0} = m_5, J_0 = m_6$ $, E_{M_0} = m_7, I_{M_0} = m_8, R_{M_0} = m_9, E_{EM_0} = m_{10}, I_{EM_0} = m_{11}, S_{V_0} = m_{12}, E_{V_0} = m_{13}, I_{V_0} = m_{14}$.

Figure 1 below Shows the schematic flow transmission dynamics described in Equation (1).

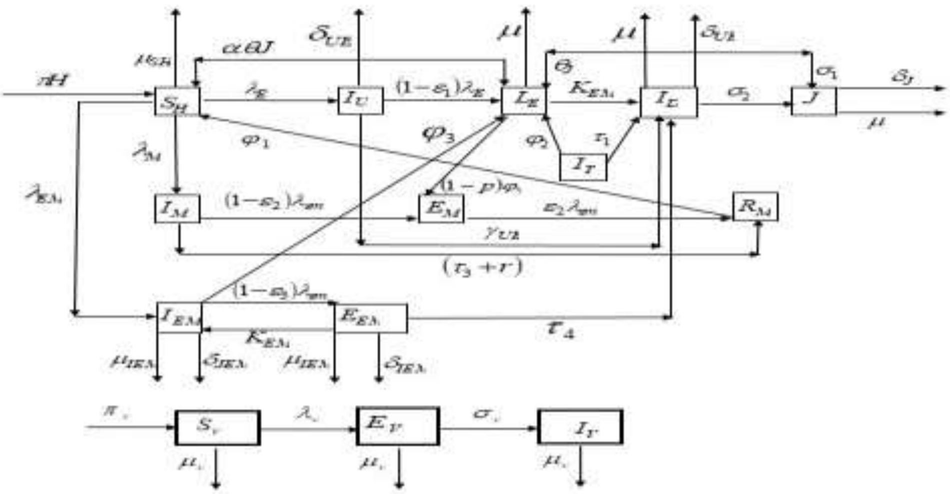

Figure 1: Schematic diagram of the Ebola-Malaria co-infection model.

D represents the fractional order Caputo's derivative and psi (ψ) represents the fractional time derivative. The model parameters in the biological context are examined alongside comprehensive explanations, including the recruitment rate of human π_H and vectors π_v, λ_M

is the force of infection for malaria transmission, λ_E is the force of infection for the Ebola virus, λ_{EM} is the force of infection of Ebola- malaria, μ is the human death rate, μ_V is the vector (mosquitoes) death rate, τ_1 is the treatment rate for Ebola, τ_2 is the malaria infected rate, τ_3 denotes Ebola virus detected, τ_4 Ebola virus exposed malaria individual, $\varepsilon_1, \varepsilon_2, \varepsilon_3$ are fraction of individual with Ebola and malaria low immunity rate and Ebola-malaria low immunity rate respectively, γ_{UE} is the detection rate of unknown Ebola virus, δ_M is the malaria induced death rate for E_M , δ_{IM} is the malaria induced death rate for I_M , σ_1 and σ_2 are the isolation rate for L_H and I_D , respectively. $\kappa_E, \kappa_M, \kappa_{EM}$ are the progression rate for malaria, Ebola, and Ebola-malaria, respectively, δ_E is Ebola induced death rate σ_V is the progression rate vectors, and ϕ is the rate of loss of immunity. β_E and β_{EM} are the effective contact rate for Ebola virus and Ebola-malaria, r is the recovery rate of malaria, λ_H and λ_V are the force of infection from vector-human and human-mosquito, respectively, ϕ_3 is the active rate of Ebola-malaria after treatment, β_M is the transmission rate from mosquito to human, β_V is the transmission rate from human to mosquito, ϕ_2 is the progression rate from I_T to the latent stage, b is the number of vector bites per unit time, ω_1 is the rate at which latent infected moves to Ebola undetected class, ρ is the rate at which treated Ebola-malaria individuals move to E_M , η_D is the modification parameter of I_D in relation to L_E η_T is the modification parameter of I_T , η_J is the modification parameter of J , η_1 and η_2 are the modification parameters of E_{EM} and I_{EM} , respectively, η_{EM} is the modification parameter of I_{EM} ,and θ is the rate at which J individuals are discharged from the treatment centers. The human population is divided into eleven classes, $S_H(t), L_E(t), I_U(t), I_D(t), I_T(t), J(t), E_M(t), I_M(t), R_M(t), E_{EM}(t), I_{EM}(t), S_V(t), E_V(t), I_V(t)$ are susceptible individuals, Ebola virus disease latently infected individuals, Ebola virus disease infected undetected Individuals, infected detected Ebola virus disease individuals , individuals under treatment for Ebola virus disease , individuals isolated for Ebola virus disease, individuals exposed to malaria disease only, individuals infected with malaria, individuals that recovered from malaria , Ebola virus disease exposed malaria Individuals, active or infected Ebola- malaria individuals, Similarly, the total vector (mosquito) population is sub-divided into susceptible mosquitoes , exposed mosquitoes and the infected mosquitoes respectively

Model Analysis

Disease-Free Equilibrium

$$E_0 = \left(\frac{\pi_H}{\mu}, 0,0,0,0,0,0,0,0,0,0, \frac{\pi_V}{\mu_V} \right)$$

Basic Reproduction Number

The basic reproduction number is calculated using the principles of the next-generation matrix, on Equation (1) above. This equation facilitates the separation of the non-negative matrix F (which represents new infection terms) and the non-singular matrix V (representing other transmission terms). This allows for the determination of the basic reproduction number, denoted as $R_0 = FV^{-1}$.

$$R_0 = \frac{\beta_{EM}((\phi_3 + \delta_{IEM} + \mu)\varepsilon_3 + (\kappa_{EM} + \delta_{IEM} + \mu + \tau_4)\eta_{EM} - \varepsilon_3\eta_{EM}\kappa_{EM} + \varepsilon_3\eta_{EM}(\kappa_{EM} + \delta_{IEM} + \mu + \tau_4)}{(\kappa_{EM} + \delta_{IEM} + \mu + \tau_4)(\phi_3 + \delta_{IEM} + \mu)}$$

An overview of the procedure of the Laplace-Adomian decomposition method.

[Olayiwola et al.(2023)] Consider a Caputo-fractional order system of differential equation given by

$${}_t^c D^\alpha \chi_n(t) = L_n(\chi_1, \chi_2, \chi_3, \cdots \chi_n) + N_n(\chi_1, \chi_2, \chi_3, \cdots \chi_n),$$

Subject to $y_n^{i_n}(0) = c_i^n$, for $n = 1,2,3 \ldots k,$ and $k_{n-1} \le \alpha \le k_n$.

From (2) ${}_t^c D^\alpha \chi_n(t)$ is the Caputo-differential of n numbers of determinable functions $\chi(t)$, and L_k, N_k respectively denotes the linear and nonlinear operators.

As illustrated in [Olayiwola et al. (2023)], the Laplace-Adomian decomposition method can be utilized to derive the solution of system by initiating the process with the Laplace transformation of equation.

$$L\left[{}_t^c D^\alpha \chi_n(t) \right] = L\left[L_n(\chi_1, \chi_2, \chi_3, \cdots \chi_n) + N_n(\chi_1, \chi_2, \chi_3, \cdots \chi_n) \right].$$

By definition 4, yields:

$$s^{\alpha_n} L[\chi_n(t)] - \sum_{i=0}^{m-1} s^{\alpha_n - i - 1} c_i^n = L\left[L_n(\chi_1, \chi_2, \chi_3, \cdots \chi_n) + N_n(\chi_1, \chi_2, \chi_3, \cdots \chi_n) \right].$$

Applying the Adomian decomposition method, the unknown functions $\chi_k(t)$ is decomposed as: $\chi_n(t) = \sum_{j=0}^{\infty} \chi_{nj}(t),$ and the nonlinear terms $N_n(\chi_1, \ldots \chi_m) = \sum_{j=0}^{\infty} X_{nj}(t), \quad n = 1,2,\ldots m$.

Where X_{nj} is the Adomian polynomial. yields:

$$L\left[\sum_{j=0}^{\infty} \chi_{nj}(t) \right] = \frac{1}{s^{\alpha_n}} \sum_{i=0}^{m-1} s^{\alpha_n - i - 1} c_i^n + \frac{1}{s^{\alpha_n}} L\left[L_n\left(\sum_{j=0}^{\infty} \chi_{1j}(t), \ldots, \sum_{j=0}^{\infty} \chi_{mj}(t) \right) \right] + \frac{1}{s^{\alpha_n}} L\left[\sum_{j=0}^{\infty} {}_{nj}(t) \right].$$

By linearity property of Laplace transform, the following recursive formula is obtained

$$L[\chi_{n0}] = \frac{1}{s^{\alpha_n}} \sum_{j=0}^{m-1} s^{\alpha_n - i - 1} c_i^n, \qquad n = 1,2,3\ldots,m \text{ ,and}$$

$$L[\chi_{n(j+1)}(t)] = \frac{1}{s^{\alpha_n}} L\left[L_n\left(\sum_{j=0}^{\infty} \chi_{1j}(t), \ldots, \sum_{j=0}^{\infty} \chi_{mj}(t) \right) \right] + \frac{1}{s^{\alpha_n}} L\left(\sum_{j=0}^{\infty} X_{nj}(t) \right).$$

Applying the inverse Laplace transform to both sides of (8) yields $\zeta_{1j}, \zeta_{2j}, \ldots \zeta_{n,j}$, $j \ge 0$ such that

$$\chi_{n0}(t) = L^{-1}\left(\frac{1}{s^{\alpha_n}} \sum_{j=0}^{m-1} s^{\alpha_n - i - 1} c_i^n \right), n = 1,2,3\ldots,m \text{ . and}$$

$$\chi_{n(j+1)}(t)=L^{-1}\left(\frac{1}{s^{\alpha_n}}L\left[\ L_n\left(\sum_{j=0}^{\infty}\chi_{1j}(t),...,\sum_{j=0}^{\infty}\chi_{mj}(t)\right)\right]+\frac{1}{s^{\alpha_n}}L\left[\sum_{j=0}^{\infty}X_{nj}(t)\right]\right).$$

Application of the Laplace Adomain Decomposition Method to the model.

Applying the Laplace transform to Equation (1) establishes a generic process with specific initial conditions. Subsequently, the Laplace inverse, along with assuming infinite series solutions, is used to derive the general model formula. This process is repeated for each component to yield Equation (2).

$$\left.\begin{aligned}
&\sum_{n=0}^{\infty}S_{H_{n+1}}(t)=L^{-1}[\frac{1}{S^{\psi_1}}L\{\pi_H-\frac{\beta_E}{N_H}(A_n+\eta_D B_n+\eta_J C_n)-\frac{\beta_{mb}}{N_v}(P_n)-\frac{\beta_{EM}}{N_H}(G_n+\eta_1 H_n+\eta_2 K_n)-\mu S_{H_n}+\phi_1 R_{M_n}+\alpha\theta J_n\}]\\
&\sum_{n=0}^{\infty}L_{E_{n+1}}(t)=L^{-1}[\frac{1}{S^{\psi_2}}L\{\varepsilon_1\frac{\beta_E}{N_H}(A_n+\eta_D B_n+\eta_J C_n)-(K_E+\sigma_1+\mu)L_{E_n}+\phi_2 I_{T_n}+(1-\alpha)\theta J_n-(1-\rho)\phi_3 I_{EM_n}\}],\\
&\sum_{n=0}^{\infty}I_{U_{n+1}}(t)=L^{-1}[\frac{1}{S^{\psi_3}}L\{(1-\varepsilon_1)\varepsilon_1\frac{\beta_E}{N_H}(A_n+\eta_D B_n+\eta_J C_n)+\omega_1 K_E L_{En}-(\gamma_{UE}+\mu+\delta_{UE})I_{D_n}\}],\\
&\sum_{n=0}^{\infty}I_{D_{n+1}}(t)=L^{-1}[\frac{1}{S^{\psi_4}}L\{(1-\omega_1)K_E L_{E_n}-(\tau_1+\mu+\delta_{ED}+\sigma_2)I_{D_n}+\gamma_{UE}I_{U_n}+\tau_4 E_{EM_n}\}],\\
&\sum_{n=0}^{\infty}I_{T_{n+1}}(t)=L^{-1}[\frac{1}{S^{\psi_5}}L\{\tau_1 I_{D_n}-(\phi_2+\mu)I_{T_n}\}],\\
&\sum_{n=0}^{\infty}J_{n+1}(t)=L^{-1}[\frac{1}{S^{\psi_6}}L\{\sigma_1 L_{nE}+\sigma_2 I_{D_n}-(\mu+\delta_J)J_n-\theta J_n\}],\\
&\sum_{n=0}^{\infty}E_{M_{n+1}}(t)=L^{-1}[\frac{1}{S^{\psi_7}}L\{\varepsilon_2\frac{\beta_{mb}}{N_v}(P_n)-(K_M+\mu)E_{M_n}-\tau_2 E_{M_n}\}],\\
&\sum_{n=0}^{\infty}I_{M_{n+1}}(t)=L^{-1}[\frac{1}{S^{\psi_8}}L\{(1-\varepsilon_2)\frac{\beta_{mb}}{N_v}(P_n)+K_M E_{M_n}-(\tau_3+r+\delta_{IM}+\mu)I_{M_n}\}],\\
&\sum_{n=0}^{\infty}R_{M_{n+1}}(t)=L^{-1}[\frac{1}{S^{\psi_9}}L\{\varepsilon_2 E_{Mn}-\tau_3 I_{M_n}+rI_{M_n}-(\phi_1+\mu)R_{M_n}\}],\\
&\sum_{n=0}^{\infty}E_{EM_{n+1}}(t)=L^{-1}[\frac{1}{S^{\psi_{10}}}L\{\varepsilon_3\frac{\beta_{EM}}{N_H}(G_n+\eta_1 H_n+\eta_2 K_n)+(K_{EM}+\delta_{JEM}+\mu)E_{EM_n}-\tau_4 E_{EM_n}\}],\\
&\sum_{n=0}^{\infty}I_{EM_{n+1}}(t)=L^{-1}[\frac{1}{S^{\psi_{11}}}L\{(1-\varepsilon_3)\frac{\beta_{EM}}{N_H}(G_n+\eta_1 H_n+\eta_2 K_n)+K_{EM}E_{EM_n}-(\phi_3+\delta_{JEM}+\mu)I_{EM_n}\}],\\
&\sum_{n=0}^{\infty}S_{V_{n+1}}(t)=L^{-1}[\frac{1}{S^{\psi_{12}}}L\{\pi_V-\frac{\beta_V b}{N_H}(M_n+\eta_1 N_n+\eta_2 O_n)-\Phi S_{V_n}\}],\\
&\sum_{n=0}^{\infty}E_{V_{n+1}}(t)=L^{-1}[\frac{1}{S^{\psi_{13}}}L\{\frac{\beta_V b}{N_H}(M_n+\eta_1 N_n+\eta_2 O_n)-(\Psi+\Phi)E_{V_n}\}],\\
&\sum_{n=0}^{\infty}I_{V_{n+1}}(t)=L^{-1}[\frac{1}{S^{\psi_{14}}}L\{\Psi E_{nV}-\Phi I_{Vn}\}].
\end{aligned}\right\}$$

By solving equation (2) and using initial condition .we obtain the following:

$$S_{H_0}=m_1, L_{E_0}=m_{2,}, I_{U_0}=m_3, I_{D_0}=m_4, I_{T_0}=m_5, J_0=m_6, E_{M_0}=m_7,$$
$$I_{M_0}=m_8, R_{M_0}=m_9, E_{EM_0}=m_{10}, I_{EM_0}=m_{11}, S_{V_0}=m_{12}, E_{V_0}=m_{13}, I_{V_0}=m_{14}. \quad (3)$$

$$S_{H_1}=(-\frac{\beta_E}{N_H}(m_3m_1+\eta_D m_4m_1+\eta_J m_6m_1)-\frac{\beta_{mb}}{N_v}(m_4m_1)-\frac{\beta_{EM}}{N_H}(m_8m_1+\eta_1 m_{10}m_1+\eta_2 m_{11}m_1)$$
$$-\mu m_1+\varphi_1 m_9+\alpha\theta m_6)\frac{t^{\psi_1}}{\Gamma(\psi_1+1)}. \quad (4)$$

$$L_{E_1} = (\varepsilon_1 \frac{\beta_E}{N_H}(m_3 m_1 + \eta_D m_4 m_1 + \eta_J m_6 m_1) - (K_E + \sigma_1 + \mu)m_2 + \varphi_2 m_5 + (1-\alpha)\theta m_6 - (1-\rho)\varphi_3 m_{11})\frac{t^{\psi_2}}{\Gamma(\psi_2 + 1)}. \quad (5)$$

$$I_{U_1} = (1-\varepsilon_1)\frac{\beta_E}{N_H}(m_3 m_1 + \eta_D m_4 m_1 + \eta_J m_6 m_1) + \omega_1 K_E m_2 - (\gamma_{UE} + \mu + \delta_{UE})m_4 \frac{t^{\psi_3}}{\Gamma(\psi_3 + 1)}.$$

$$I_{D_1} = ((1-\omega_1)K_E m_2 - (\tau_1 + \mu + \delta_{ED} + \sigma_2)m_4 + \gamma_{UE} m_4 + \tau_4 m_{10})\frac{t^{\psi_4}}{\Gamma(\psi_4 + 1)}. \quad (7)$$

$$I_{T_1} = (\tau_1 m_4 - (\varphi_2 + \mu)m_5)\frac{t^{\psi_5}}{\Gamma(\psi_5 + 1)}. \quad (8)$$

$$J_1 = (\sigma_1 m_2 + \sigma_2 m_4 - (\mu + \delta_J)m_6 - \theta m_6)\frac{t^{\psi_6}}{\Gamma(\psi_6 + 1)}. \quad (9)$$

$$E_{M_1} = \varepsilon_2 \frac{\beta_{mb}}{N_v}(m_4 m_1) - (K_M + \mu)m_7 - \tau_2 m_7)\frac{t^{\psi_7}}{\Gamma(\psi_7 + 1)}. \quad (10)$$

$$I_{M_1} = ((1-\varepsilon_2)\frac{\beta_{mb}}{N_v}(m_4 m_1) + K_M m_7 - (\tau_3 + r + \delta_{IM} + \mu)m_8)\frac{t^{\psi_8}}{\Gamma(\psi_8 + 1)}. \quad (11)$$

$$R_{M_1} = (\varepsilon_2 m_7 - \tau_3 m_8 + r m_8 - (\varphi_1 + \mu)m_9)\frac{t^{\psi_9}}{\Gamma(\psi_9 + 1)}. \quad (12)$$

$$E_{EM_1} = (\varepsilon_3 \frac{\beta_{EM}}{N_H}(m_8 m_1 + \eta_1 m_{10} m_1 + \eta_2 m_{11} m_1) + (K_{EM} + \delta_{JEM} + \mu)m_{10} - \tau_4 m_{10})\frac{t^{\psi_{10}}}{\Gamma(\psi_{10} + 1)}. \quad (13)$$

$$I_{EM_1} = (1-\varepsilon_3)\frac{\beta_{EM}}{N_H}(m_8 m_1 + \eta_1 m_{10} m_1 + \eta_2 m_{11} m_1) + K_{EM} m_{10} - (\varphi_3 + \delta_{JEM} + \mu)m_{11})\frac{t^{\psi_{11}}}{\Gamma(\psi_{11} + 1)}. \quad (14)$$

$$S_{V_1} = (\pi_V - K_4(m_8 m_{12} + \eta_1 m_{10} m_{12} + \eta_2 m_{11} m_{12}) - \Phi m_{12})\frac{t^{\psi_{12}}}{\Gamma(\psi_{12} + 1)}. \quad (15)$$

$$E_{V_1} = (K_4((m_8 m_{12} + \eta_1 m_{10} m_{12} + \eta_2 m_{11} m_{12}) - (\Psi + \Phi)m_{13})\frac{t^{\psi_{13}}}{\Gamma(\psi_{13} + 1)}. \quad (16)$$

$$\begin{aligned}
S_{H_2} &= (-\frac{\beta_E}{N_H}((m_3)(\pi_H - \frac{\beta_E}{N_H}(m_3 m_1 + \eta_D m_4 m_1 + \eta_J m_6 m_1) \\
&- \frac{\beta_{mb}}{N_v}(m_4 m_1) - \frac{\beta_{EM}}{N_H}(m_8 m_1 + \eta_1 m_{10} m_1 + \eta_2 m_{11} m_1) - \mu m_1 + \varphi_1 m_9 + \alpha\theta m_6)\frac{t^{2\psi_1}}{\Gamma(2\psi_1 + 1)}) \\
&+ (m_1)((1-\varepsilon_1)\frac{\beta_E}{N_H}(m_3 m_1 + \eta_D m_4 m_1 + \eta_J m_6 m_1) + \omega_1 K_E m_2 - (\gamma_{UE} + \mu + \delta_{UE})m_4 \frac{t^{\psi_3 + \psi_1}}{\Gamma(\psi_3 + \psi_1 + 1)}) \\
&+ \eta_D((m_1)(((1-\omega_1)K_E m_2 - (\tau_1 + \mu + \delta_{ED} + \sigma_2)m_4 + \gamma_{UE} m_4 + \tau_4 m_{10})\frac{t^{\psi_4 + \psi_1}}{\Gamma(\psi_4 + \psi_1 + 1)}) \\
&+ (m_4)((\pi_H - \frac{\beta_E}{N_H}(m_3 m_1 + \eta_D m_4 m_1 + \eta_J m_6 m_1) - \frac{\beta_{mb}}{N_v}(m_4 m_1) \qquad (17) \\
&- \frac{\beta_{EM}}{N_H}(m_8 m_1 + \eta_1 m_{10} m_1 + \eta_2 m_{11} m_1) - \mu m_1 + \varphi_1 m_9 + \alpha\theta m_6)\frac{t^{2\psi_1}}{\Gamma(2\psi_1 + 1)})
\end{aligned}$$

$$+\eta_J((m_1)((\sigma_1 m_2+\sigma_2 m_4-(\mu+\delta_J)m_6-\theta m_6)\frac{t^{\psi_6+\psi_1}}{\Gamma(\psi_6+\psi_1+1)}+(m_6)((\pi_H-\frac{\beta_E}{N_H}(m_3m_1+\eta_D m_4 m_1+\eta_J m_6 m_1))$$
$$-\frac{\beta_{mb}}{N_v}(m_4m_1)-\frac{\beta_{EM}}{N_H}(m_8m_1+\eta_1 m_{10}m_1+\eta_2 m_{11}m_1)-\mu m_1+\varphi_1 m_9+\alpha\theta m_6)\frac{t^{2\psi_1}}{\Gamma(2\psi_1+1)}))$$
$$+\eta_1((m_1)((\varepsilon_3\frac{\beta_{EM}}{N_H}(m_8m_1+\eta_1 m_{10}m_1+\eta_2 m_{11}m_1)+(K_{EM}+\delta_{JEM}+\mu)m_{10}-\tau_4 m_{10})\frac{t^{\psi_{10}+\psi_1}}{\Gamma(\psi_{10}+\psi_1+1)})$$
$$+(m_{10})((\pi_H-\frac{\beta_E}{N_H}(m_3m_1+\eta_D m_4m_1+\eta_J m_6m_1)-\frac{\beta_{mb}}{N_v}(m_4m_1)-\frac{\beta_{EM}}{N_H}(m_8m_1+\eta_1 m_{10}m_1+\eta_2 m_{11}m_1)$$
$$-\mu m_1+\varphi_1 m_9+\alpha\theta m_6)\frac{t^{2\psi_1}}{\Gamma(2\psi_1+1)})$$

$$L_{E_2}=\varepsilon_1\frac{\beta_E}{N_H}((m_3)(\pi_H-\frac{\beta_E}{N_H}(m_3m_1+\eta_D m_4m_1+\eta_J m_6m_1)$$
$$-\frac{\beta_{mb}}{N_v}(m_4m_1)-\frac{\beta_{EM}}{N_H}(m_8m_1+\eta_1 m_{10}m_1+\eta_2 m_{11}m_1)-\mu m_1+\varphi_1 m_9+\alpha\theta m_6)\frac{t^{\psi_1+\psi_2}}{\Gamma(\psi_1+\psi_2+1)})$$
$$+(m_1)((1-\varepsilon_1)\frac{\beta_E}{N_H}(m_3m_1+\eta_D m_4m_1+\eta_J m_6m_1)+\omega_1 K_E m_2-(\gamma_{UE}+\mu+\delta_{UE})m_4\frac{t^{\psi_3+\psi_2}}{\Gamma(\psi_3+\psi_2+1)})$$
$$-\frac{\beta_{EM}}{N_H}(m_8m_1+\eta_1 m_{10}m_1+\eta_2 m_{11}m_1)-\mu m_1+\varphi_1 m_9+\alpha\theta m_6)\frac{t^{\psi_1+\psi_2}}{\Gamma(\psi_1+\psi_2+1)})$$
$$+\eta_J((m_1)((\sigma_1 m_2+\sigma_2 m_4-(\mu+\delta_J)m_6-\theta m_6)\frac{t^{\psi_6+\psi_2}}{\Gamma(\psi_6+\psi_2+1)})-(K_E+\sigma_1+\mu)((\varepsilon_1\frac{\beta_E}{N_H}(m_3m_1+\eta_D m_4m_1+\eta_J m_6m_1)$$
$$-(K_E+\sigma_1+\mu)m_2+\varphi_2 m_5+(1-\alpha)\theta m_6-(1-\rho)\varphi_3 m_{11})\frac{t^{2\psi_2}}{\Gamma(2\psi_2+1)})$$
$$+\varphi_2((\tau_1 m_4-(\varphi_2+\mu)m_5)\frac{t^{\psi_5+\psi_2}}{\Gamma(\psi_5+\psi_2+1)})+(1-\alpha)\theta((\sigma_1 m_2+\sigma_2 m_4-(\mu+\delta_J)m_6-\theta m_6)\frac{t^{\psi_6+\psi_2}}{\Gamma(\psi_6+\psi_2+1)})$$
$$-(1-\rho)\varphi_3(((1-\varepsilon_2)\frac{\beta_{mb}}{N_v}(m_4m_1)+K_M m_7-(\tau_3+r+\delta_{IM}+\mu)m_8)\frac{t^{\psi_8+\psi_2}}{\Gamma(\psi_8+\psi_2+1)}). \quad (18)$$

$$I_{U_2}=(1-\varepsilon_1)\varepsilon_1\frac{\beta_E}{N_H}(((m_3)(\pi_H-\frac{\beta_E}{N_H}(m_3m_1+\eta_D m_4m_1+\eta_J m_6m_1)-\frac{\beta_{mb}}{N_v}(m_4m_1)-\frac{\beta_{EM}}{N_H}(m_8m_1+\eta_1 m_{10}m_1$$
$$+\eta_2 m_{11}m_1)-\mu m_1+\varphi_1 m_9+\alpha\theta m_6)\frac{t^{\psi_1+\psi_3}}{\Gamma(\psi_1+\psi_3+1)})+(m_1)((1-\varepsilon_1)\frac{\beta_E}{N_H}(m_3m_1+\eta_D m_4m_1+\eta_J m_6m_1)$$
$$+\omega_1 K_E m_2-(\gamma_{UE}+\mu+\delta_{UE})m_4\frac{t^{2\psi_3}}{\Gamma(2\psi_3+1)})+\eta_D((m_1)(((1-\omega_1)K_E m_2-(\tau_1+\mu+\delta_{ED}+\sigma_2)m_4+\gamma_{UE}m_4$$
$$+\tau_4 m_{10})\frac{t^{\psi_4+\psi_3}}{\Gamma(\psi_4+\psi_3+1)})+(m_4)((\pi_H-\frac{\beta_E}{N_H}(m_3m_1+\eta_D m_4m_1+\eta_J m_6m_1)-\frac{\beta_{mb}}{N_v}(m_4m_1)-\frac{\beta_{EM}}{N_H}(m_8m_1$$
$$+\eta_1 m_{10}m_1+\eta_2 m_{11}m_1)-\mu m_1+\varphi_1 m_9+\alpha\theta m_6)\frac{t^{\psi_1+\psi_3}}{\Gamma(\psi_1+\psi_3+1)})+\eta_J((m_1)((\sigma_1 m_2+\sigma_2 m_4-(\mu+\delta_J)m_6$$
$$-\theta m_6)\frac{t^{\psi_6+\psi_3}}{\Gamma(\psi_6+\psi_3+1)})-\frac{\beta_{EM}}{N_H}(m_8m_1+\eta_1 m_{10}m_1+\eta_2 m_{11}m_1)-\mu m_1+\varphi_1 m_9+\alpha\theta m_6)\frac{t^{\psi_1+\psi_3}}{\Gamma(\psi_1+\psi_3+1)})))$$
$$+\omega_1 K_E(((\varepsilon_1\frac{\beta_E}{N_H}(m_3m_1+\eta_D m_4m_1+\eta_J m_6m_1)-(K_E+\sigma_1+\mu)m_2+\varphi_2 m_5+(1-\alpha)\theta m_6-(1-\rho)\varphi_3$$
$$m_{11})\frac{t^{\psi_2+\psi_3}}{\Gamma(\psi_2+\psi_3+1)}))-(\gamma_{UE}+\mu+\delta_{UE})(((1-\omega_1)K_E m_2-(\tau_1+\mu+\delta_{ED}+\sigma_2)m_4+\gamma_{UE}m_4+$$
$$\tau_4 m_{10})\frac{t^{\psi_4+\psi_3}}{\Gamma(\psi_{14}+\psi_3+1)} \quad (19)$$

$$I_{T_2} = \tau_1(((1-\omega_1)K_E m_2 - (\tau_1 + \mu + \delta_{ED} + \sigma_2)m_4 + \gamma_{UE} m_4 + \tau_4 m_{10})\frac{t^{\psi_4+\psi_5}}{\Gamma(\psi_4+\psi_5+1)}) - (\varphi_2+\mu)((\tau_1 m_4 - (\varphi_2+\mu)m_5)\frac{t^{2\psi_5}}{\Gamma(2\psi_5+1)}). \tag{20}$$

$$J_2 = \sigma_1((\varepsilon_1 \frac{\beta_E}{N_H}(m_3m_1 + \eta_D m_4 m_1 + \eta_J m_6 m_1) - (K_E + \sigma_1 + \mu)m_2 + \varphi_2 m_5 + (1-\alpha)\theta m_6 - (1-\rho)\varphi_3 m_{11})\frac{t^{\psi_2+\psi_6}}{\Gamma(\psi_2+\psi_6+1)}) + \sigma_2(((1-\omega_1)K_E m_2 - (\tau_1+\mu+\delta_{ED}+\sigma_2)m_4 + \gamma_{UE}m_4 + \tau_4 m_{10})\frac{t^{\psi_4+\psi_6}}{\Gamma(\psi_4+\psi_6+1)}) - (\mu+\delta_J)((\sigma_1 m_2 + \sigma_2 m_4 - (\mu+\delta_J)m_6 - \theta m_6)\frac{t^{2\psi_6}}{\Gamma(2\psi_6+1)}) - \theta(\sigma_1 m_2 + \sigma_2 m_4 - (\mu+\delta_J)m_6 - \theta m_6)\frac{t^{2\psi_6}}{\Gamma(2\psi_6+1)}) \tag{21}$$

$$E_{M_2} = \varepsilon_2 \frac{\beta_{mb}}{N_v}(((m_1)((\sigma_V m_{12} - \mu_V m_{14})\frac{t^{\psi_{14}+\psi_7}}{\Gamma(\psi_{14}+\psi_7+1)}) + (m_{14})((\pi_H - \frac{\beta_E}{N_H}(m_3m_1 + \eta_D m_4 m_1 + \eta_J m_6 m_1) - \frac{\beta_{mb}}{N_v}(m_4m_1) - \frac{\beta_{EM}}{N_H}(m_8m_1 + \eta_1 m_{10} m_1 + \eta_2 m_{11} m_1) - \mu m_1 + \varphi_1 m_9 + \alpha\theta m_6)\frac{t^{\psi_1+\psi_7}}{\Gamma(\psi_1+\psi_7+1)}))) - (K_M+\mu)((\varepsilon_2\frac{\beta_{mb}}{N_v}(m_4m_1) - (K_M+\mu)m_7 - \tau_2 m_7)\frac{t^{2\psi_7}}{\Gamma(2\psi_7+1)} - \tau_2(\varepsilon_2\frac{\beta_{mb}}{N_v}(m_4m_1) - (K_M+\mu)m_7 - \tau_2 m_7)\frac{t^{2\psi_7}}{\Gamma(2\psi_7+1)}) \tag{22}$$

$$I_{M_2} = (1-\varepsilon_2)\frac{\beta_{mb}}{N_v}(((m_1)((\sigma_V m_{12} - \mu_V m_{14})\frac{t^{\psi_{14}+\psi_8}}{\Gamma(\psi_{14}+\psi_8+1)}) + (m_{14})((\pi_H - \frac{\beta_E}{N_H}(m_3m_1 + \eta_D m_4 m_1 + \eta_J m_6 m_1) - \frac{\beta_{mb}}{N_v}(m_4m_1) - \frac{\beta_{EM}}{N_H}(m_8m_1 + \eta_1 m_{10}m_1 + \eta_2 m_{11}m_1) - \mu m_1 + \varphi_1 m_9 + \alpha\theta m_6)\frac{t^{\psi_1+\psi_8}}{\Gamma(\psi_1+\psi_8+1)})) + K_M(\varepsilon_2\frac{\beta_{mb}}{N_v}(m_4m_1) - (K_M+\mu)m_7 - \tau_2 m_7)\frac{t^{\psi_7+\psi_8}}{\Gamma(\psi_7+\psi_8+1)}) - (\tau_3 + r + \delta_{IM} + \mu)((1-\varepsilon_2)\frac{\beta_{mb}}{N_v}(m_4m_1) + K_M m_7 - (\tau_3 + r + \delta_{IM} + \mu)m_8)\frac{t^{2\psi_8}}{\Gamma(2\psi_8+1)} \tag{23}$$

$$R_{M_2} = \varepsilon_2(\varepsilon_2 \frac{\beta_{mb}}{N_v}(m_4m_1) - (K_M + \mu)m_7 - \tau_2m_7)\frac{t^{\psi_7+\psi_9}}{\Gamma(\psi_7+\psi_9+1)}) - \tau_3((1-\varepsilon_2)\frac{\beta_{mb}}{N_v}(m_4m_1)$$
$$+ K_M m_7 - (\tau_3 + r + \delta_{IM} + \mu)m_8)\frac{t^{\psi_8+\psi_9}}{\Gamma(\psi_8+\psi_9+1)} + r((1-\varepsilon_2)\frac{\beta_{mb}}{N_v}(m_4m_1) + K_M m_7 - (\tau_3 + r \quad (24)$$
$$+ \delta_{IM} + \mu)m_8)\frac{t^{\psi_8+\psi_9}}{\Gamma(\psi_8+\psi_9+1)} - (\varphi_1+\mu)(\varepsilon_2 m_7 - \tau_3 m_8 + rm_8 - (\varphi_1+\mu)m_9)\frac{t^{2\psi_9}}{\Gamma(2\psi_9+1)}$$

$$E_{EM_2} = \varepsilon_3 \frac{\beta_{EM}}{N_H}((m_1)(((1-\varepsilon_2)\frac{\beta_{mb}}{N_v}(m_4m_1) + K_M m_7 - (\tau_3 + r + \delta_{IM} + \mu)m_8)\frac{t^{\psi_8+\psi_{10}}}{\Gamma(\psi_8+\psi_{10}+1)})$$
$$+ (m_8)(\pi_H - \frac{\beta_E}{N_H}(m_3m_1 + \eta_D m_4m_1 + \eta_J m_6m_1) - \frac{\beta_{mb}}{N_v}(m_4m_1) - \frac{\beta_{EM}}{N_H}(m_8m_1 + \eta_1 m_{10}m_1 + \eta_2 m_{11}m_1)$$
$$- \mu m_1 + \varphi_1 m_9 + \alpha\theta m_6)\frac{t^{\psi_1+\psi_{10}}}{\Gamma(\psi_1+\psi_{10}+1)} + \eta_1((m_1)((\varepsilon_3 \frac{\beta_{EM}}{N_H}(m_8m_1 + \eta_1 m_{10}m_1 + \eta_2 m_{11}m_1) \quad (25)$$
$$+ (K_{EM} + \delta_{JEM} + \mu)m_{10} - \tau_4 m_{10})\frac{t^{2\psi_{10}}}{\Gamma(2\psi_{10}+1)}) + (m_{10})((\pi_H - \frac{\beta_E}{N_H}(m_3m_1 + \eta_D m_4m_1 + \eta_J m_6m_1)$$
$$- \frac{\beta_{mb}}{N_v}(m_4m_1) - \frac{\beta_{EM}}{N_H}(m_8m_1 + \eta_1 m_{10}m_1 + \eta_2 m_{11}m_1) - \mu m_1 + \varphi_1 m_9 + \alpha\theta m_6)\frac{t^{\psi_1+\psi_{10}}}{\Gamma(\psi_1+\psi_{10}+1)}$$
$$+ (m_{11})((\pi_H - \frac{\beta_E}{N_H}(m_3m_1 + \eta_D m_4m_1 + \eta_J m_6m_1) - \frac{\beta_{mb}}{N_v}(m_4m_1) - \frac{\beta_{EM}}{N_H}(m_8m_1 + \eta_1 m_{10}m_1 + \eta_2 m_{11}m_1)$$
$$- \mu m_1 + \varphi_1 m_9 + \alpha\theta m_6)\frac{t^{\psi_1+\psi_{10}}}{\Gamma(\psi_1+\psi_{10}+1)}) + (K_{EM} + \delta_{JEM} + \mu)(\varepsilon_3 \frac{\beta_{EM}}{N_H}(m_8m_1 + \eta_1 m_{10}m_1 + \eta_2 m_{11}m_1)$$
$$+ \eta_2((m_1)((1-\varepsilon_3)\frac{\beta_{EM}}{N_H}(m_8m_1 + \eta_1 m_{10}m_1 + \eta_2 m_{11}m_1) + K_{EM} m_{10} - (\varphi_3 + \delta_{JEM} + \mu)m_{11})\frac{t^{\psi_{11}+\psi_{10}}}{\Gamma(\psi_{11}+\psi_{10}+1)}))$$

$$- \tau_4(\varepsilon_3 \frac{\beta_{EM}}{N_H}(m_8m_1 + \eta_1 m_{10}m_1 + \eta_2 m_{11}m_1) + (K_{EM} + \delta_{JEM} + \mu)m_{10} - \tau_4 m_{10})\frac{t^{2\psi_{10}}}{\Gamma(2\psi_{10}+1)})$$

$$+ \eta_1((m_1)((\varepsilon_3 \frac{\beta_{EM}}{N_H}(m_8m_1 + \eta_1 m_{10}m_1 + \eta_2 m_{11}m_1) + (K_{EM} + \delta_{JEM} + \mu)m_{10} - \tau_4 m_{10})\frac{t^{\psi_{10}+\psi_{11}}}{\Gamma(\psi_{10}+\psi_{11}+1)})$$
$$+ (m_{10})((\pi_H - \frac{\beta_E}{N_H}(m_3m_1 + \eta_D m_4m_1 + \eta_J m_6m_1) - \frac{\beta_{mb}}{N_v}(m_4m_1) - \frac{\beta_{EM}}{N_H}(m_8m_1 + \eta_1 m_{10}m_1 + \eta_2 m_{11}m_1)$$
$$- \mu m_1 + \varphi_1 m_9 + \alpha\theta m_6)\frac{t^{\psi_1+\psi_{11}}}{\Gamma(\psi_1+\psi_{11}+1)} \quad (26)$$
$$+ \eta_2((m_1)((1-\varepsilon_3)\frac{\beta_{EM}}{N_H}(m_8m_1 + \eta_1 m_{10}m_1 + \eta_2 m_{11}m_1) + K_{EM} m_{10} - (\varphi_3 + \delta_{JEM} + \mu)m_{11})\frac{t^{2\psi_{11}}}{\Gamma(2\psi_{11}+1)})$$
$$+ (m_{11})((\pi_H - \frac{\beta_E}{N_H}(m_3m_1 + \eta_D m_4m_1 + \eta_J m_6m_1) - \frac{\beta_{mb}}{N_v}(m_4m_1) - \frac{\beta_{EM}}{N_H}(m_8m_1 + \eta_1 m_{10}m_1 + \eta_2 m_{11}m_1)$$
$$- \mu m_1 + \varphi_1 m_9 + \alpha\theta m_6)\frac{t^{\psi_1+\psi_{11}}}{\Gamma(\psi_1+\psi_{11}+1)}) + K_{EM}(\varepsilon_3 \frac{\beta_{EM}}{N_H}(m_8m_1 + \eta_1 m_{10}m_1 +$$
$$\eta_2 m_{11}m_1) + (K_{EM} + \delta_{JEM} + \mu)m_{10} - \tau_4 m_{10})\frac{t^{\psi_{10}+\psi_{11}}}{\Gamma(\psi_{10}+\psi_{11}+1)})$$
$$- (\varphi_3 + \delta_{JEM} + \mu)((1-\varepsilon_2)\frac{\beta_{mb}}{N_v}(m_4m_1) + K_M m_7 - (\tau_3 + r + \delta_{IM} + \mu)m_8)\frac{t^{\psi_8+\psi_{11}}}{\Gamma(\psi_8+\psi_{11}+1)}$$

$$S_{V_2} = (-K_4((m_8)(\pi_V - K_4(m_8 m_{12} + \eta_1 m_{10} m_{12} + \eta_2 m_{12}) - \Phi m_{12})\frac{t^{2\psi_{12}}}{\Gamma(2\psi_{12}+1)} + (m_{12})((1-\varepsilon_2)K_2(m_4 m_1)$$
$$+ K_M m_7 - (\tau_3 + r + \delta_{IM} + \mu)m_8 \frac{t^{\psi_8+\psi_{12}}}{\Gamma(\psi_8+\psi_{12}+1)} + \eta_1((m_{10})(\pi_V - K_4(m_8 m_{12} + \eta_1 m_{10} m_{12} + \eta_2 m_{12})$$
$$-\Phi m_{12})\frac{t^{2\psi_{12}}}{\Gamma(2\psi_{12}+1)} + (m_{12})(\varepsilon_3 K_2(m_8 m_1 + \eta_1 m_{10} m_1 + \eta_2 m_{11} m_1) + (K_{EM} + \delta_{JEM} + \mu)m_{10} \tag{27}$$
$$-\tau_4 m_{10})\frac{t^{\psi_{10}+\psi_{12}}}{\Gamma(\psi_{10}+\psi_{12}+1)}) + \eta_2((m_{11})(\pi_V - K_4(m_8 m_{12} + \eta_1 m_{10} m_{12} + \eta_2 m_{12}) - \Phi m_{12})\frac{t^{2\psi_{12}}}{\Gamma(2\psi_{12}+1)}$$
$$+(m_{12})((1-\varepsilon_3)K_2(m_8 m_1 + \eta_1 m_{10} m_1 + \eta_2 m_{11} m_1) + K_{EM} m_{10} - (\varphi_3 + \delta_{JEM} + \mu)m_{11})\frac{t^{\psi_{11}+\psi_{12}}}{\Gamma(\psi_{11}+\psi_{12}+1)})$$
$$-\Phi(\pi_V - K_4(m_8 m_{12} + \eta_1 m_{10} m_{12} + \eta_2 m_{12}) - \Phi m_{12})\frac{t^{2\psi_{12}}}{\Gamma(2\psi_{12}+1)}$$

$$E_{V_2} = K_4((m_8)(\pi_V - K_4(m_8 m_{12} + \eta_1 m_{10} m_{12} + \eta_2 m_{12}) - \Phi m_{12})\frac{t^{\psi_{12}+\psi_{13}}}{\Gamma(\psi_{12}+\psi_{13}+1)} + (m_{12})((1-\varepsilon_2)$$
$$K_2(m_4 m_1) + K_M m_7 - (\tau_3 + r + \delta_{IM} + \mu)m_8 \frac{t^{\psi_8+\psi_{13}}}{\Gamma(\psi_8+\psi_{13}+1)} + \eta_1((m_{10})(\pi_V - K_4 \tag{28}$$
$$(m_8 m_{12} + \eta_1 m_{10} m_{12} + \eta_2 m_{12}) - \Phi m_{12})\frac{t^{\psi_{12}+\psi_{13}}}{\Gamma(\psi_{12}+\psi_{13}+1)} + (m_{12})(\varepsilon_3 K_2(m_8 m_1 + \eta_1 m_{10} m_1 +$$

$$\eta_2 m_{11} m_1) + (K_{EM} + \delta_{JEM} + \mu)m_{10} - \tau_4 m_{10})\frac{t^{\psi_{10}+\psi_{13}}}{\Gamma(\psi_{10}+\psi_{13}+1)}) + \eta_2((m_{11})(\pi_V - K_4(m_8 m_{12} +$$
$$\eta_1 m_{10} m_{12} + \eta_2 m_{12}) - \Phi m_{12})\frac{t^{\psi_{12}+\psi_{13}}}{\Gamma(\psi_{12}+\psi_{13}+1)} + (m_{12})((1-\varepsilon_3)K_2(m_8 m_1 + \eta_1 m_{10} m_1 + \eta_2 m_{11} m_1)$$
$$+ K_{EM} m_{10} - (\varphi_3 + \delta_{JEM} + \mu)m_{11})\frac{t^{\psi_{11}+\psi_{13}}}{\Gamma(\psi_{11}+\psi_{13}+1)}) - (\Psi + \Phi)(K_4((m_8 m_{12} + \eta_1 m_{10} m_{12} + \eta_2 m_{11} m_{12})$$
$$-(\Psi + \Phi)m_{13})\frac{t^{2\psi_{13}}}{\Gamma(2\psi_{13}+1)})$$

$$I_{V_2} = \Psi(K_4((m_8 m_{12} + \eta_1 m_{10} m_{12} + \eta_2 m_{11} m_{12}) - (\Psi + \Phi)m_{13})\frac{t^{\psi_{13}+\psi_{14}}}{\Gamma(\psi_{13}+\psi_{14}+1)}$$
$$-\Phi(\Psi m_{12} - \Phi m_{14})\frac{t^{2\psi_{14}}}{\Gamma(2\psi_{14}+1)} \tag{29}$$

Results

Numerical simulations in this section use the Laplace Adomian Decomposition Method (LADM) to analyze a fractional-order model with the Caputo-derivative operator. Simulations consider predetermined initial conditions and parameter values specified, we achieve the subsequent series solution with flexibility in choosing the order of approximation;

$$S_H = 13800 - \frac{28508.0400 t^{\psi}}{\Gamma(\psi+1)} + \frac{2.98855620510^7 t^{2\psi}}{\Gamma(2\psi+1)}$$

$$L_E = -1043.02972 - \frac{15296.33720 t^{\psi}}{\Gamma(\psi+1)} - \frac{1.05614754310^7 t^{2\psi}}{\Gamma(2\psi+1)}$$

$$I_U = 200 - \frac{53.35680000t^{\psi}}{\Gamma(\psi+1)} + \frac{7.99817258210^7 t^{2\psi}}{\Gamma(2\psi+1)}$$

$$I_D = 300 + \frac{93.1400t^{\psi}}{\Gamma(\psi+1)} - \frac{2018.441440t^{2\psi}}{\Gamma(2\psi+1)} \quad I_T = 350 + \frac{118.7900t^{\psi}}{\Gamma(\psi+1)} + \frac{24.38860200t^{2\psi}}{\Gamma(2\psi+1)}$$

$$J = 180 + \frac{1440.200t^{\psi}}{\Gamma(\psi+1)} - \frac{10847.65143t^{2\psi}}{\Gamma(2\psi+1)}$$

$$E_M = 2000 - \frac{490.6400000t^{\psi}}{\Gamma(\psi+1)} + \frac{4.14322237310^5 t^{2\psi}}{\Gamma(2\psi+1)}$$

$$I_M = 9000 - \frac{1225.0600000t^{\psi}}{\Gamma(\psi+1)} + \frac{4.1433106310^5 t^{2\psi}}{\Gamma(2\psi+1)}$$

$$R_M = 7500 + \frac{858.3000t^{\psi}}{\Gamma(\psi+1)} - \frac{219.9462220t^{2\psi}}{\Gamma(2\psi+1)} \quad E_{EM} = 700 + \frac{29939.56600t^{\psi}}{\Gamma(\psi+1)} - \frac{2.839655940t^{2\psi}}{\Gamma(2\psi+1)}$$

$$I_{EM} = 100 + \frac{13304.40400t^{\psi}}{\Gamma(\psi+1)} - \frac{2.74210131210^8 t^{2\psi}}{\Gamma(2\psi+1)}$$

$$S_V = 1304.00 + \frac{204.070400t^{\psi}}{\Gamma(\psi+1)} + \frac{9.92727975910^6 t^{2\psi}}{\Gamma(2\psi+1)}$$

$$E_V = 700 + \frac{40.9296000t^{\psi}}{\Gamma(\psi+1)} - \frac{8.52558794410^5 t^{2\psi}}{\Gamma(2\psi+1)} \quad I_V = 500 + \frac{65.00t^{\psi}}{\Gamma(\psi+1)} - \frac{93.65864380t^{2\psi}}{\Gamma(2\psi+1)}$$

Taking the $\psi = 0.65$ $\psi = 0.85$ and $\psi = 1$ in above expressions to obtain the graphs and table 1 below, showcasing numerical values.

Table1: Presenting numerical values.

Class	t=0	t=0.1	t=0.2	t=0.3	t=0.4	t=0.5
$S_H(t)$	13800	160377.01	605809.63	1.35× 10 6	2.39× 10 6	3.74× 10 6
$L_E(t)$	1043.03	-55380.04	-215331.81	-480898.33	-852079.60	-1.33× 10 6
$I_U(t)$	200	400103.29	1.6× 10 6	3.6× 10 6	6.40× 10 6	9.99× 10 6
$I_D(t)$	300	299.22	278.26	237.11	175.78	94.26
$I_T(t)$	350	362.00	374.25	386.73	399.47	412.44
$J(t)$	180	269.78	251.09	123.92	-111.73	-455.86
$E_M(t)$	2000	4022.55	10188.32	20497.37	34949.52	53544.96
$I_M(t)$	9000	10949.15	17041.61	27277.38	41656.46	60178.85
$R_M(t)$	7500	7584.73	7667.26	7747.59	7825.72	7901.66
$E_{EM}(t$	700	-1.42× 10 6	-5.67× 10 6	-1.28× 10 7	-2.27× 10 7	-3.55× 10 7
$I_{EM}(t)$	100	-1.34× 10	-5.48× 10 6	-1.23× 10 7	-2.19× 10 7	-3.43× 10 7
$S_V(t)$	1304.00	50961.31	199891.41	448094.31	795570.01	1.24× 10 6
$E_V(t)$	700	-3558.71	-16342.99	-37652.87	-67488.33	-105849.38
$I_V(t)$	500	506.03	511.13	515.29	518.51	520.79

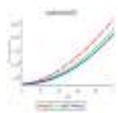	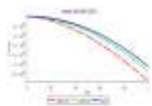
Figure 2: Behavior of Susceptible SH(t) at different values of fractional order Psi	**Figure 3:** Behavior of Latently L[E](t) values of fractional order Psi
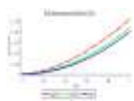	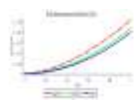
Figure 4: Behavior of Ebola affected unnoticed I[U](t) at different values of fractional order Psi	**Figure 5**: Behavior of Infected detected I[D](t) at different values of fractional order Psi

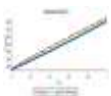

Figure 6: Behavior of Treatment [T](t) at different values of fractional order Psi

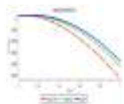

Figure 7: Behavior of Isolated [J](t) at different values of fractional order Psi

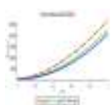

Figure 8: Behavior of Exposed malaria E[M](t) at different values of fractional order Psi

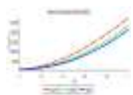

Figure 9: Behavior of infected with malaria I[M](t) at different values of fractional order Psi

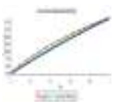

Figure 10: Behavior of Recovered from malaria R[M](t) at different values of fractional order Psi

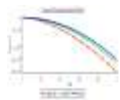

Figure 11: Behavior of Exposed Ebola Malaria E[EM](t) at different values of fractional order Psi

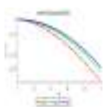

Figure 12: Behavior of Infected Ebola Malaria I[EM](t) at different values of fractional order Psi

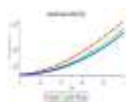

Figure 13: Behavior of Susceptible mosquito S[V](t) at different values of fractional order Psi

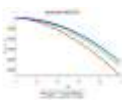	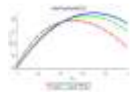
Figure 14: Behavior of Exposed Mosquito E[V](t) at Different Values of Fractional order Psi	**Figure 15**: Behavior of Exposed mosquito E[V](t) at different values of fractional order Psi

Graph analysis

The behavior of a fractional-order Ebola-malaria model is represented in Figures 2 to 15. This model incorporates fractional derivatives, allowing for a more flexible and accurate representation of the dynamics of the disease compared to traditional derivative-based models.

- **Figures 2 and 3:** These figures show how the fractional order affects the decline in susceptible and latent dynamics. Higher values of the fractional order (psi) result in slower declines in susceptibility, mainly due to the transmission rate (psi). Similarly, latent dynamics show that higher psi values lead to slower dynamics at integer order and faster dynamics at fractional order.
- **Figures 4 to 9:** These figures illustrate the conversion from exposure to infection and how it varies with different fractional orders. Slower rates are observed at lower fractional orders, while faster rates are observed at higher fractional orders. The model examines various populations related to Ebola and malaria, all showing growth in integer order, highlighting the effectiveness of contact interventions.
- **Figures 10 and 11:** Figure 10 demonstrates how recovery from malaria increases with treatment, particularly showing a fractional increase corresponding to a higher number of individuals recovering. Figure 11 indicates that the exposed population of Ebola-malaria grows faster in integer order, suggesting rapid protection.
- **Figures 12 and 13:** Figure 12 analyzes the impact of contact rates on infected cases of Ebola-malaria, showing that a higher rate of infection occurs as the fractional order increases. Figure 13 reveals a decrease in mosquito susceptibility as the fractional order increases, indicating higher treatment effectiveness.
- **Figures 14 and 15:** These figures show the dynamic effects of fractional orders on the behavior of exposed and infected mosquitoes. They indicate a reduction in infected mosquitoes as the fractional value increases, emphasizing the importance of fractional modeling in capturing the intricacies of mosquito behavior in the context of the disease.

In summary, the use of fractional order modeling allows for a more nuanced understanding of the dynamics of the Ebola-malaria model. Different figures highlight how changing the fractional order (psi) impacts various aspects of the disease, including susceptibility, latency, conversion from exposure to infection, recovery, contact rates, and mosquito behavior. These insights are essential for fine-tuning disease control strategies and understanding the effects of treatment and interventions on disease dynamics.

Convergence analysis.

The result is a series that converges quickly and reliably to the given answer. We assess the convergence of the series employing conventional techniques with reference to the framework proposed by Yunus et al. (2023).

Theorem 1.Let Y be a Banach space and $P: Y \to Y$ be a contractive nonlinear operator such that for all $y, y^1 \in Y, // T(Y) - T(Y^1) \leq k // y - y^1 //, 0 < k < 1.$ Then T has a unique point y such that $Ty = y,$ where $y = (S, L, T, J, R).$ The series given in (14) can be written by applying Adomian decomposition method as:

$$y_m = Ty_{m-1}, y_{m-1} = \sum y_i \ m = 1,2,3,\ldots,$$

and assume that $y_0 \in B_r(y)$ $B_r(y)=$

Proof. For (i), using mathematical induction for $m = 1$,we have $\|y_0 - y\| = \|T(y_0) - T(y)\| \leq k\|y_0 - y\|.$

Let the result is true for $n = 1,$ then $\|y_0 - y\| \leq k^{n-1}\|y_0 - y\|.$

We have $y_n - y = T(y_{n-1}) - T(y) \leq k\, y_{n-1} - y \leq k^n\, y_n - y$. i.e.
$\|y_n - y\| \leq k^n \|y_0 - y\| \leq k^n r < r$ Which implies that $y_m \in B$.

(ii) Since $\|y_n - y\| \leq k^n \|y_0 - y\|$ and as $\lim_{n \to \infty} k^n = 0,$ therefore, we have $\lim_{n \to \infty} \|y_n - y\| = 0 \Rightarrow \lim_{n \to \infty} y_m = y$

Discussion

The Laplace-Adomian decomposition method has proven itself to be an invaluable tool in the realm of public health research, particularly when tackling fractional-order models and augmenting the Ebola-Malaria model. This methodology offers a means of generating adaptable solutions for epidemiological models that incorporate fractional orders. While it's important to note that the study predominantly employs shorter time periods to prevent the occurrence of negative population figures, the potential for enhanced accuracy looms large when dealing with extended temporal scopes and original datasets. Additionally, one of the notable advantages of this method is its ability to validate singular solutions within the model. This validation is not to be underestimated, as it plays a pivotal role in bolstering the management of disease outbreaks. In essence, the Laplace-Adomian decomposition method shows remarkable promise when it comes to delivering precise solutions for fractional-order mathematical models in the context of public health research. Now, let's delve into the fractional-order Ebola-Malaria model, meticulously depicted across Figures 1 to 14. These figures embrace fractional derivatives, thereby endowing the model with enhanced flexibility and accuracy compared to its traditional counterparts. The key findings extracted from these graphical representations are truly enlightening. Figures 1 and 2 conspicuously illustrate how elevating the fractional order results in a deceleration of the decline in susceptibility and latent dynamics. This phenomenon can be predominantly attributed to transmission rates (commonly represented as psi). Turning our attention to Figures 3 to 8, they unveil how the shift from exposure to infection is subject to variations based on fractional orders. Slower rates prevail at lower fractional orders, while higher fractional orders engender a hastening effect. Notably, contact interventions exhibit their effectiveness in influencing various population segments tied to Ebola and malaria. Figures 9 and 10 bring to light the fact that recovery from malaria experiences an upswing in response to treatment. Furthermore, the exposed population within the context of Ebola-Malaria grows at an accelerated pace in integer-order settings, indicating swift protection. Figures 11 and 12 offer a profound analysis of how contact rates impact the number of infected cases and the susceptibility of mosquitoes. These figures reveal that higher fractional orders correlate with increased infection rates and heightened treatment efficacy. Finally, Figures 13 and 14 underscore the dynamic consequences that fractional orders have on exposed and infected mosquitoes. As the fractional value increases, there's a noticeable reduction in the number of infected mosquitoes. This underscores the critical role of fractional modeling in our quest to comprehend mosquito behavior within the broader spectrum of disease dynamics. In summary, fractional-order modeling offers a nuanced and multifaceted lens through which we can understand the intricate dynamics of the Ebola-Malaria model. These figures collectively illustrate the profound impact of adjusting the fractional order (psi) on susceptibility, latency, exposure-to-infection conversion, recovery, contact rates, and mosquito behavior. These insights are of paramount importance when it comes to refining disease control strategies and comprehending the ramifications of treatment and interventions within the complex landscape of disease dynamics.

Conclusion

The Laplace-Adomian decomposition method plays a crucial role in infectious disease studies, particularly in the context of the Ebola-Malaria model. It allows for a more in-depth analysis of disease dynamics through fractional-order modeling. The flexibility and precision of this method are valuable for understanding diseases influenced by various factors like population density, climate, and demographics. The fractional-order Ebola-Malaria model, as represented in Figures 1 to 14, demonstrates the significance of using fractional derivatives in epidemiological models. These figures provide valuable insights into the behavior of the disease dynamics under different fractional orders (psi). They show that the choice of psi affects susceptibility, latent dynamics, and exposure to infection conversion, recovery rates, contact rates, and mosquito behavior. This nuanced understanding can help in tailoring disease control strategies and assessing the impact of treatments and interventions. Overall, the Laplace-Adomian decomposition method and fractional order modeling are promising tools in public health research. However, researchers should exercise caution, especially when working with short periods, to avoid negative population numbers. Longer periods and original data can enhance the accuracy of the models, making them more applicable in real-world scenarios. These tools contribute to our understanding of infectious diseases and aid in the development of effective prevention and treatment strategies.

Recommendations

Additional fractional derivatives, like the variational iteration approach, expand fractional calculus in infectious disease studies. Computational assessments improve our understanding of complex systems. Incorporating numerical methods such as the homotopy perturbation method and homotopy analysis method with real data enhances precision. While the Caputo fractional order derivative and Laplace Adomian decomposition methods are effective, further improvement is possible. Real-world data increases accuracy and validity by refining parameters and validating predictions. These approaches enhance our understanding of infectious diseases and assist in prevention and treatment strategies. Continuous exploration and refinement are necessary for advancing infectious disease modeling.

Acknowledgements

The authors hereby acknowledge by thanking everyone who has contributed to the success of this research.

Reference

Abdilraze A, and Pelinosky D 2011 Convergence of the Adomian decomposition method for initial value problem, *Numer. Methods. Part. Diff. Equations* 27 749-766.

Ahmed I, Baba IA, Yusuf A, Kumam P, and Kumam W 2020 Analysis of Caputo fractional-order model for COVID-19 with lockdown. *Adv. Differ. Equ.* 394(2020). https://doi.org/ 10.1186/s13662-020-02853-0

Alaje AI, Morufu OO, Adedokun KA, Adedeji JA, Oladapo AO 2022 Modified Homotopy perturbation method and its application to analytical solitons of fractional-order Korteweg–de Vries equation, *Beni-Suef Univ. J. Basic Appl. Sci.*11:139 https://doi.org/10.1186/ s43088-022-00317-

Ali, Rabiei F, Shah K, Khodadadi T 2021 Qualitative analysis of fractal-fractional order COVID-19 mathematical model with case study of Wuhan, Alexandria Eng. J. 60: 477–489

Amir YA, Mashdy AMS, Shwayaa RT, Youssef ESM 2018 Laplace transform method for solving nonlinear biochemical reaction model and nonlinear Emden Fowler system. *J. Eng. Appl. Sci*. 13(17):7388-7394.

Arqub OA and Ajou El 2013 Solution of the fractional epidemic model by Homotopy analysis method. *J. King Saud Univ. Sci.* 25(1), 73-81.

Bahaa GM 2017 Fractional optimal control problem for differential system with delay argument. *Adv Differ Equation* 69: https://doi.org/10.1186/s13662-017-1121-6

Chakraverty S, Jena RM and Jena SK 2020 *Time-fractional order biological systems* *with uncertain parameters*. Cham, Switzerland: Springer.

Dokuyucu and Dutta 2020 A fractional order model for Ebola Virus with the new Caputo fractional derivative without singular kernel *Chaos, Solitons Fractals* 134: 109717.

Haq F, Shah K, Rahman G, Shahzad M 2018 Numerical solution of fractional order smoking model via laplace Adomian decomposition method. *Alexandria Eng. J.* 57: 1061–1069.

Hassan, Al-Zoubi, Freihet, Al-Smadi, and Momani 2019 Solution of fractional SIR epidemic model using residual power series method. *Appl. Math. Inform. Sci.* 13(2): 153-161.

Matsebula L and Nyabadza F 2022 Mathematical analysis of cholera typhoid co-infection transmission dynamics. *Front. Appl. Math. Stat.* 8:892098.

Mahdy, AM, Higazy, M, and Mohamed, MS (2021). Optimal and memristor-based control of a nonlinear fractional tumor-immune model. *Comput. Mater Continua* 67(3): 3463-3486.

Mashdy AMS 2022 A numerical method for solving the nonlinear equation of Emden-Fowler Models J. Ocean Eng. Sci. http://doi.org\10.1016\j.joes.2022.04.019.

Mtisi E, Rwezaura H and Tchuenche J M 2009 A mathematical analysis of malaria and tuberculosis co-dynamics. *Discrete Contin. Dynam. Syst.-B* 12(4), 827-864.

Muhammad F,Ali A, Merve TT, Muhammad M, Aqeel A, Emad EM and Ibrahim

SY 2022 Fractal fractional-Order derivative for HIV/AID model with mittag-Leffler kernel. *Alexandria Eng. J.* 61: 10965-10980.

Mutua JM, Wang FB and Vaidya NK 2015 Modeling malaria and typhoid fever co-infection dynamics. *Math. Biosci.* 264: 128-144.

Mukandavire Z, Gumel AB, Garira W and Tchuenche JM 2009 Mathematical analysis of a model for HIV-malaria co-infection. *Math. Biosci. Eng.* 6(2): 333-362.

Ndaïrou F and Torres DF 2021 Mathematical analysis of a fractional COVID-19 model applied to Wuhan, Spain and Portugal. *Axioms* 10(3): 135.

Oguntolu FA, Yavalah CF, Udom TA, Ayoola AA, Victor 2022 A Mathematical Modelling of Lymphatic Filariasis and Malaria Co-infection. http://repository.futminna.edu.ng:8080/ jspui/handle/123456789/15380.

Olayiwola MO, Alaje AI, Olarewaju AY and Adedokun KA 2023 A caputo fractional order epidemic model for evaluating the effectiveness of high-risk quarantine and vaccination strategies on the spread of COVID-19. *Healthcare Anal.* 3:100179.

Omoloye MA and Adewale SO. 2021 Mathematical Analysis of Sensitive Parameters on the Dynamical Transmission of Ebola-Malaria Co-infections. *IJCSIS.* 19*:*7.

Pinto CM and Machado JT 2013 Fractional model for malaria transmission under control strategies. *Comput. Math. Appl.* 66(5): 908-916.

Reiner JRC, Perkins TA, Barker CM, Niu T, Chaves LF, Ellis AM and Smith DL 2013 a systematic review of mathematical models of mosquito-borne pathogen transmission: 1970–2010. *J. R. Soc., Interface* 10(81): 20120921.

Sinan and Khan 2020 Analytic approximate solution of rabies transmission dynamics using homotopy perturbation method. *Matrix Sci. Math.* 4(1): 01- 05.

Yunus AO, Olayiwola MO., Omoloye MA and Oladapo AO 2023 A fractional order model of Lassa disease using the Laplace-adomian decomposition method. *Healthcare Anal.* 100167. https://doi.org/10.1016/j.health.2023.100167.

Yunus AO, Olayiwola MO, Adedokun KA, Adedeji JA and Alaje IA 2022 Mathematical analysis of fractional-order Caputo's derivative of coronavirus disease model via Laplace Adomian decomposition method. *Beni-Suef Univ. J. Basic Appl. Sci.* 11(1): 144.